Acta Mech 201, 37–46 (2008)
DOI 10.1007/s00707-008-0071-1

Leen van Wijngaarden · Christian Veldhuis

On hydrodynamical properties of ellipsoidal bubbles

Dedicated to Professor Wilhelm Schneider on the occasion of his 70th birthday

Received: 29 January 2008 / Revised: 27 February 2008 / Published online: 7 August 2008

Abstract A major part of this paper is taken up by the calculation of the first axisymmetric surface oscillation frequency and the (2, 0) mode of an ellipsoidal bubble, in order to compare with experimentally obtained values of bubbles rising in water. First, an energy method is used for an ellipsoid oscillating in stagnant water. Interestingly, with help of a paper by Bjerknes [12] at 1873!. The results compare poorly with experiments. Agreement improves when the oscillation of the rise velocity is taken into account. The remaining difference between the results of theory and experimental values is ascribed to deviation of the bubble shape from an ellipsoid. Finally, volume oscillations of ellipsoidal bubbles are calculated with the energy method and the results compare well with those of an earlier work, based on an electrical analogon.

1 Introduction

With pleasure we contribute to this Festschrift for Professor Wilhelm Schneider at the occasion of his 70th birthday. Wilhelm Schneider and one of us (L.v.W) worked together many years in the Scientific Council of CISM in Udine, Italy.We share an interest in classical hydrodynamics and I hope that this contribution will please him. We wish him many years to come in good health.

This paper is on gas bubbles rising in clean water, so clean that there are no surfactants. Then, the boundary condition on the interface between gas and liquid is that the tangential shear stress must vanish. Rising in water under buoyancy, very small bubbles (diameter of order of 0.1 mm) remain spherical, but with diameters of 1 mm and larger they assume a shape which is approximately an oblate ellipsoid [1] with the short axis pointing in vertical direction. The ratio of the larger axis to the minor one, indicated here with χ, depends on the speed of rising which in turn depends on the size and on liquid properties. The terminal speed of rise, U_T, is often expressed in terms of the Reynolds number Re , defined as

$$Re = U_T D_{\mathrm{eq}}/\nu, \tag{1}$$

where D_{eq} is the equivalent bubble diameter and ν the kinematic viscosity of the liquid. The axes ratio depends on the Weber number We defined as

$$We = \rho U_T^2 D_{\mathrm{eq}}/\sigma, \tag{2}$$

where ρ and σ are the water density and air–water surface tension, respectively. Below $D_{\mathrm{eq}} = 1.8\,\mathrm{mm}$ ($Re \sim 600$), bubbles rise rectilinearly, above that value they describe a spiraling or zigzagging path [2,3], but

L. van Wijngaarden (✉)
J. M. Burgers Centre for Fluid Dynamics, University of Twente, Enschede, The Netherlands
E-mail: l.vanwijngaarden@tnw.utwente.nl

C. Veldhuis
Maritime Research Institute in the Netherlands, Wageningen, The Netherlands

the shape remains undisturbed [4]. This changes at a still larger diameter of 2.8 mm. Shape oscillations start to occur here. These oscillations, studied before in [5–7] and other papers, formed part of the thesis [8] of the junior author. The oscillations can be characterized with the indices n and m, where n is the number of wave lengths in the direction from pole to pole and m the same in azimuthal (equatorial) direction. In particular the (n, m) values of shape oscillations and their frequencies were measured, see [8,9] . When searching the literature with the intention to compare the observed frequencies with theoretically obtained ones, we found that little is known. For a sphere these frequencies are well known and are given in [10] for example. For an ellipsoid it is different. In [7] a numerical calculation is made of eigenmodes of rising bubbles. An analytical approach would be welcome. In [6] an approximate calculation is given, which will be discussed later in the paper. Here we attempt an exact calculation, for an ellipsoidal shape, in the spirit of the classical calculation of the modes for a spherical shape. This consists in first calculating the kinetic energy associated with a certain mode. During oscillation the kinetic energy fluctuates and continuously kinetic energy is transformed in surface energy and vice-versa. Averaged over a cycle of the particular mode, these energies must be the same. From this equality the frequency of that particular mode is obtained. In the following we shall go through this derivation.

2 Potential flow caused by an oscillating ellipsoid

We consider an oblate axisymmetric ellipsoid, with major axis a and minor axis c. The (2,0) mode is one in which c and a change in such a way that the volume (for the breathing mode in which the volume changes, see Sect. 8) remains constant. We denote the radius of a sphere with the same volume with r_{eq} and the volume, apart from a factor $4/3\pi$, with V,

$$V = a^2 c = r_{\mathrm{eq}}^3. \tag{3}$$

The ellipsoid is immersed in an inviscid and incompressible liquid which is at rest at infinity. We want to calculate the kinetic energy of the liquid when c is performing a periodic oscillation with respect to an undisturbed c_0,

$$c - c_0 = \Delta \cos \omega t, \tag{4}$$

where t means time and ω is the desired frequency, to be calculated. One would expect that the potential for this motion can be found in textbooks on hydrodynamics. This, however, is not the case. In [10,11] the potential for uniform motion of an ellipsoid is given , but not for the type of motion considered here. We have, however, been able to construct the desired potential with help of a paper [12], by Bjerknes published in 1873! Let in a cartesian x, y, z frame the ellipsoid be given by

$$\frac{x^2}{a^2} + \frac{y^2}{b^2} + \frac{z^2}{c^2} = 1. \tag{5}$$

We shall later restrict to an axisymmetric ellipsoid where the semi- axes a and b are the same, but keep the discussion temporarily general. Let c execute oscillations as given in Eq. (4) keeping V, as given in Eq. (3), constant. We expect that the natural, that is without external excitation, frequency comes close to an eigenmode of the ellipsoid, which in turn is close to the shape of a bubble. According to [12] the potential has the form

$$\phi = K \left\{ \int_{\lambda}^{\infty} G(a, b, c) \left[\left(\frac{x^2}{s + a^2} + \frac{y^2}{s + b^2} + \frac{z^2}{s + c^2} \right) F^{-1} \right] \mathrm{d}s \right\}. \tag{6}$$

In this expression

$$F^{-1}(s) = \frac{1}{\left(1 + s/a^2\right)^{1/2} \left(1 + s/b^2\right)^{1/2} \left(1 + s/c^2\right)^{1/2}}, \tag{7}$$

$$G(a, b, c) = a\partial/\partial a + b\partial/\partial b - 2c\partial/\partial c, \tag{8}$$

and the parameter λ is the positive root of the equation

$$\frac{x^2}{\lambda + a^2} + \frac{y^2}{\lambda + b^2} + \frac{z^2}{\lambda + c^2} - 1 = 0. \tag{9}$$

The prefactor -2 in the last term at the right hand side of Eq. (8) differs from that in the preceding terms, involving a and b, due to the condition of constant volume. K is a constant to be determined by the boundary condition. Equation (9) represents a family of confocal ellipsoids . The meaning of λ is that with given x, y and z, the ellipsoid through this point has the label λ. In particular, the ellipsoid that we are considering, given in Eq. (5), has the label $\lambda = 0$. Caution is needed in applying the operator in Eq. (8). For the axisymmetric ellipsoid, a may be put equal to b *after* differentiation, but not before. In other relations the equality may be introduced directly as long as no differentiation with respect to a, b or c is involved. So, to find K we write, in cylindrical coordinates, the ellipsoid as

$$H(r, z, t) = \frac{r^2}{a^2} + \frac{z^2}{c^2} - 1 = 0. \tag{10}$$

The normal to this is

$$\boldsymbol{n} = \nabla H / |\nabla H| \ . \tag{11}$$

The boundary condition is that on $H = 0$

$$\nabla\phi.\boldsymbol{n} = \frac{-\partial H/\partial t}{\nabla H}. \tag{12}$$

In applying Eq. (12) to Eq. (10) we must take, with a view to the condition of constant volume,

$$\dot{a} = -\frac{1}{2}\frac{a\dot{c}}{c} = \dot{b}. \tag{13}$$

Evaluating the right hand side of Eq. (12) with help of Eq. (10) , the boundary condition on the potential becomes

$$\nabla\phi.\boldsymbol{n} = \frac{\left(3z^2/c^2 - 1\right) a/2\,(\dot{c}/c)}{\left\{1 + \left(\chi^2 - 1\right) z^2/c^2\right\}^{1/2}}. \tag{14}$$

The reader is reminded that χ is the ratio a/c. We impose this condition on the potential in Eq. (6) in $\lambda = 0$. We need the derivatives of λ with respect to r and z. These are obtained from Eq. (9), thereby taking $a = b$ and $x^2 + y^2 = r^{2\cdot}$. We obtain

$$K = \frac{\dot{a}}{4a\,(1+J)} = -\frac{\dot{c}}{8\mathrm{c}\,(1+J)}, \tag{15}$$

with

$$J = \int_0^\infty \left\{\frac{1}{2}\left(a\frac{\partial}{\partial a} + b\frac{\partial}{\partial b}\right) - c\frac{\partial}{\partial c}\right\}\left\{\frac{F^{-1}}{s+a^2}\right\}\mathrm{d}s. \tag{16}$$

In Eq. (16) F^{-1} is as given at the right hand side of Eq. (7). It can be verified that, with K, from Eq. (15), inserted in Eq. (6), ϕ satisfies the potential equation and also the boundary condition, Eq. (14). There is an interesting difference here with the usual way to determine this type of natural frequencies for a sphere. The usual way, see e.g. [13], is to disturb the surface with a series of spherical harmonics of small amplitude. To second order in the small quantity, there is a volume change going with this which manifests itself in a $1/(x^2 + y^2 + z^2)^{1/2}$ behaviour at infinity. A correction is needed then. In our treatment the volume remains constant during the perturbation. From Eqs. (6)–(9) it follows that for $\lambda \to \infty$, which corresponds, see Eq. (9), with $\left(x^2 + y^2 + z^2\right)^{1/2} \to \infty$,

$$\phi \sim \int_\lambda^\infty \frac{x^2 + y^2 + z^2}{s^{7/2}}\mathrm{d}s \sim \frac{1}{\left(x^2 + y^2 + z^2\right)^{3/2}},$$

where Eq. (9) has been used. This means that for either of the variables $x.y$, z becoming very large the potential behaves like that of a quadrupole situated in the origin. This is as it should be since there is no volume change, nor a resultant velocity, which is associated with a dipole.

We now calculate the kinetic energy in the liquid ,

$$E_k = -\rho/2 \oint \phi \nabla\phi . \mathbf{n} \mathrm{d}S, \tag{17}$$

where the integration is over the surface of the ellipsoid with elementary surface dS,

$$\mathrm{d}S = 2\pi\,(Vc)^{1/2} \left\{1 + \left(\chi^2 - 1\right) \frac{z^2}{c}\right\}^{1/2} \mathrm{d}\frac{z}{c}. \tag{18}$$

Using Eqs. (6), and (14) –(18), we obtain after quite some integration and algebraical manipulations,

$$E_k = 2\pi\rho V \left(\frac{\dot{c}}{c}\right)^2 \frac{1}{32\,(1+J)} \int_{-1}^{1} \left(\frac{3z^2}{c^2} - 1\right) \left\{2\mathrm{J}\left(x^2 + y^2\right) - 4Jz^2\right\} \mathrm{d}\frac{z}{c}.$$

Carrying out the integration over z results for the kinetic energy in

$$E_k = -2\pi\rho V \dot{c}^2 \frac{J(\chi^2 + 2)}{30\,(1+J)}. \tag{19}$$

Evaluation of J, as given in Eq. (16), gives

$$\begin{aligned} J &= -\int_0^\infty \frac{1}{F} \left\{\frac{a^2}{(s+a^2)^2} + \frac{s}{\left(s+a^2\right)\left(s+c^2\right)} - \frac{s}{(s+a^2)^2}\right\} \mathrm{d}s \\ &= -\frac{3}{2}\chi^2 \frac{\left(\chi^2+2\right)\cos^{-1}\chi^{-1} - 3\left(\chi^2-1\right)^{1/2}}{\left(\chi^2-1\right)^{5/2}}. \end{aligned} \tag{20}$$

The value of J for $\chi = 1$ can easier be obtained from the intermediate result and is

$$J = -\int_0^\infty \frac{a^5}{(s+a^2)^{7/2}} = -\frac{2}{5}.$$

For all values of χ of interest, $\chi \geq 1$, J is negative and hence E_k positive as it should be.

3 Calculation of surface energy

Periodically kinetic energy is turned into surface energy. Let the surface tension be σ , and let the undisturbed surface be of magnitude S_0. Integration of Eq. (18) gives for arbitrary c

$$S = 2\pi \left\{\frac{V}{c} + \frac{1}{2}c^2 \left(\frac{V}{V-c^3}\right)^{1/2} \ln \frac{1 + \left(\frac{V-c^3}{V}\right)^{1/2}}{1 - \left(\frac{V-c^3}{V}\right)^{1/2}}\right\}. \tag{21}$$

This can be written in many other ways. This one is convenient, because V remains constant during the considered motion. With a perturbation of c as described in Eq. (4), we can express the fluctuating surface energy $E_\sigma = S - S_0$ as

$$E_\sigma = 2\pi\sigma \left[\left(\frac{\mathrm{d}S}{\mathrm{d}c}\right)_0 (c - c_0) + \frac{1}{2}\left(\left(\frac{\mathrm{d}^2 S}{\mathrm{d}c^2}\right)_0 (c - c_0)^2 + \cdots\right)\right]. \tag{22}$$

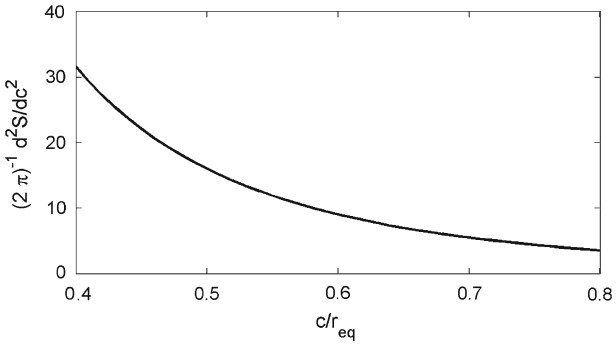

Fig. 1 The expression $\frac{1}{2\pi}\frac{\mathrm{d}^2 S}{\mathrm{d}c^2}$, as occurring in Eq. (21) as a function of $\frac{c}{r_{\mathrm{eq}}} = \chi^{-2/3}$

Averaged over a cycle, the first term in brackets vanishes, and the first contribution comes from the second term, which we denote with $E_{\sigma,2}$. Since E_k is expressed in Eq. (19) in terms of the axis ratio χ , it useful to do the same for $E_{\sigma,2}$. With $c/r_{\mathrm{eq}} = \chi^{-2/3}$, we obtain from Eqs. (20) and (21)

$$\frac{E_{\sigma,2}}{2\pi\sigma\,(c-c_0)^2} = \left\{ \begin{array}{l} \chi^2 + \frac{1}{2}\ln\left\{ \frac{1+\left(\frac{\chi^2-1}{\chi^2}\right)^{1/2}}{1-\left(\frac{\chi^2-1}{\chi^2}\right)^{1/2}} \right\} \left(1 + \frac{9}{2(\chi^2-1)} + \frac{27}{8}\frac{1}{(\chi^2-1)^2}\right)\left(\frac{\chi^2}{\chi^2-1}\right)^{1/2} - \\ \frac{\chi^2}{\chi^2-1}\left(\frac{3}{2} + \frac{9}{8(\chi^2-1)}\right) \end{array} \right\}. \quad (22.1)$$

Figure 1 is a graph of $1/2\pi\,\frac{\mathrm{d}^2 S}{\mathrm{d}c^2}$ as a function of c/r_{eq}, $\chi^{-2/3}$ in terms of the axes ratio.

4 The (2,0) mode frequency

The frequency ω follows from averaging E_k, from Eq. (19), and E_σ, from Eq. (22), over a cycle when c is subjected to a fluctuation as is given in Eq. (4). In [8,9] experiments are described with bubbles of several mm radius in purified water. Regarding surface oscillations, measured values of both $\omega/2\pi$ and χ are reported for a number of bubble sizes. Figure 2 , from [8], shows experimental values. The dots are measured values of the (2.0) mode frequency. As shown in Fig. 2, both the vertical velocity changes and the vortex shedding frequencies in the wake correspond with the (2.0) mode. In the experiments also the (2.2) mode is clearly present, which corresponds with a non axisymmetric surface oscillation and does not concern us here. In the measured spectra reported in [8] the (2.0) and (2.2) modes are dominant. Other frequencies are not to any significant intensity visible.

The general tendency is that the frequency of the (2.0) mode is decreasing with the bubble size. This tendency is less clear, but still well visible, when the presentation is in dimensionless form, the frequency

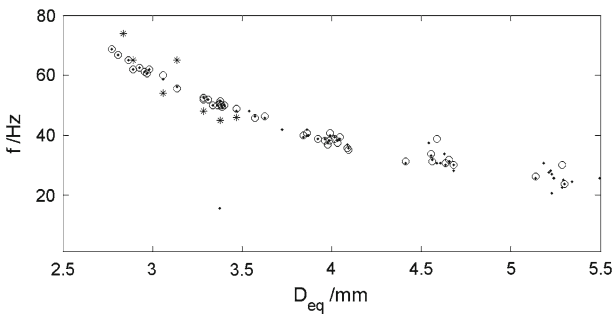

Fig. 2 Frequencies obtained from experiments in purified water; *bullet* refers to the (2,0) mode, *circle* to fluctuation of vertical velocity. The *asterisk* are vortex shedding frequencies in the wake. Note that both *circle* and *asterisk* follow the (2,0) mode. From [8]

Table 1 Calculated and measured bubble oscillation frequencies for (2.0) mode

r_{eq} (mm)	U_T (m/s)	χ	ω_{theory} (rad/s) $x(\rho r_{eq}^3/\sigma)^{1/2}$	$\omega_{theor,corrected}$ $x(\rho r_{eq}^3/\sigma)^{1/2}$	ω_{expt} (rad/s) $x(\rho r_{eq}^3/\sigma)^{1/2}$	Meiron
3.9	0.26	2.3	5.3	4.9	2.6	2.8
5.5	0.29	2.7	5.6	4.4	2.4	2.7

being rendered dimensionless with $(\rho r_{eq}^3/\sigma)^{1/2}$ and the axis ratio χ instead of the equivalent radius. In Table 1 we give some experimental values, as given in [8].

Apparently, the calculated values, fourth column, although of the right order of magnitude, are larger than the measured ones, last column. Also, and for the moment we focus on that, we see that the experimental values decrease with χ whereas the calculated ones increase. The trend in the experimental values is also observed in other experiments, see [8].

It is useful to inspect in this connection the expressions for E_k and $S - S_0$. For χ values of interest here $J/1+J$ in Eq. (19) is about -0.7. Further it follows from inspection of the graph in Fig. 1 that $(1/4\pi)d^2S/dc^2$ is roughly equal to χ^2. Then, it follows from Eqs. (19) and (22) that , upon averaging,

$$\omega \sim 6.5\sqrt{\frac{\chi^2}{2+\chi^2}}\left(\sigma/\rho r_{eq}^3\right)^{1/2}. \tag{23}$$

Indeed, for the values 2.3 and 2.7 of χ , Eq. (23) gives 5.5 and 5.8 times $\left(\sigma/\rho r_{eq^3}\right)^{1/2}$ respectively, close to the exact values in Table 1. The approximation in Eq. (23) clearly shows that in our theory the dimensionless frequency increases with χ, in contrast to experiment.

The main reason for this is the following. We have assumed the ellipsoid to be immersed in a fluid at rest at infinity. However, in the experimental situation the bubble rises under buoyancy and in a reference frame attached to the bubble, the fluid at infinity moves with the rise velocity. The ellipsoidal shape results precisely from the pressure distribution produced by this motion. During the oscillatory motion the virtual mass of the bubble changes periodically. The viscous relaxation time $r_{eq}^2/18\,\nu$ is for bubble sizes of interest of the order of 1 *sec*, whereas a typical period of oscillation is 50–100 times smaller, see Fig. 2. This means that the impulse I, defined by

$$I = MU, \tag{24}$$

remains constant during an oscillation, because viscosity can be neglected on that time scale. In Eq. (24) the quantity M is the virtual mass and U the rise velocity. M is for a body of arbitrary shape a tensor, but in our case, where the body is axisymmetric and moves along the symmetry axis, a scalar quantity. Without surface oscillations, the velocity is U_T and the added mass M_0, say, Then, during an oscillation the velocity changes, which has been observed earlier and been brought in connection with added mass changes in [14] . Figure 2 clearly shows that the frequency of the vertical velocity fluctuation coincides with that of the (2,0) mode. The associated energy fluctuation has to be taken into account. This is the subject of the next section.

5 Fluctuating vertical motion

With constant impulse $M_o U_T$, the velocity fluctuates according to

$$U = \frac{M_0}{M}U_T. \tag{25}$$

The added mass M is , see [11],

$$M = 2/3\pi r_{eq}^3 \frac{2\gamma}{2-\gamma}, \tag{26}$$

where γ is an integral of the type that we have already met,

$$\gamma = \int_0^\infty \frac{a^2 c\,ds}{(s+a^2)(s+c^2)^{3/2}} = \frac{2\chi^2}{\chi^2-1}\left\{1 - \frac{1}{(\chi^2-1)^{1/2}}\cos^{-1}\chi\right\}. \tag{27}$$

The quantity $2\gamma/2-\gamma$, drawn in [15] as function of χ, shows clearly a linear behaviour accurately described by $-0.132+A\chi$, with $A=1.13$. Using this we write instead of Eq. (26)

$$M=2/3\pi\rho r_{\mathrm{eq}}^3(-0.132+A\chi). \tag{28}$$

After these preliminaries, we consider the kinetic energy , associated with the vertical motion,

$$E_v=1/2MU^2=1/2(M_0U_T)U. \tag{29}$$

It is important to note that in this case the kinetic energies associated with the vertical motion and the shape oscillations, represented by Eq. (6), are additive. The potentials, ϕ_1 and ϕ_2, say, are additive anyway , but in writing down the surface integral for the resulting kinetic energy, similar to Eq. (17), it appears that the mixed terms $\phi_1\nabla\phi_2.\boldsymbol{n}$ and $\phi_2\nabla\phi_1.\boldsymbol{n}$ give no contribution.

Under small variations of the shorter axis c, described in Eq. (4), E_v can be written, with help of Eq. (25)

$$\frac{1}{2}\left(M_0U_{T^2}\right)\frac{M_0}{M_0+\left(\frac{\mathrm{d}M}{\mathrm{d}c}\right)_0(c-c_0)+\frac{1}{2}\left(\frac{\mathrm{d}^2M}{\mathrm{d}c^2}\right)_0(c-c_0)^2+\cdots}$$

Expanding the fraction gives for the coefficient of $(c-c_0)^2$

$$\frac{1}{M_{0^2}}\left(\frac{\mathrm{d}M}{\mathrm{d}c}\right)_0^2-\frac{1}{2}\left(\frac{\mathrm{d}^2M}{\mathrm{d}c^2}\right)_0\frac{1}{M_0}. \tag{30}$$

Using Eq. (28) to find these derivatives, we must, in differentiating χ with respect to c, keep in mind that the volume, $4/3\pi a^2c$, remains constant. We obtain finally for the quantity preceding $(c-c_0)^2$ in the expansion of E_v

$$E_v-(E_v)_0=E_v^*=\frac{1}{2}\left(\frac{2}{3}\pi\right)\rho U_{T^2}A\chi r_{\mathrm{eq}}^3\frac{3}{8c_0^2}(c-c_0)^2. \tag{31}$$

6 Energy balance and renewed calculation of ω

Averaged over a period of the (2,0) surface oscillation, the energy balance is

$$\langle E_k\rangle+\langle E_v^*\rangle=\langle E_\sigma\rangle, \tag{32}$$

where E_k, E_v^*, and E_σ are given in Eqs. (19), (31) and (22), respectively, and $\langle\,\rangle$ means averaging over time. The surface energy is, just as the right hand side of Eq. (31), proportional to $(c-c_0)^2$. In order to compare their relative magnitude we consider

$$\frac{E_v^*}{\sigma}=(2\pi)\left(\frac{\rho U_T^2r_{\mathrm{eq}}}{\sigma}\right)\frac{A}{16}\chi^{7/3}(c-c_0)^2. \tag{33}$$

To write the right hand side of Eq. (31) in this form, we have used Eq. (3). In the second pair of brackets at the right hand side of Eq. (33) we recognize the Weber number based upon r_{eq}, one half of the Weber number *We* defined in Eq. (2). Therefore we write , with $A=1.13$,

$$\frac{E_v^*}{\sigma}=2\pi We\frac{1.13}{32}\chi^{7/3}(c-c_0)^2. \tag{34}$$

For the experiments mentioned in Table 1 *We* can be calculated using the given values of U_T. For the $\chi=2.4$ case $We=3.9$ and for $\chi=2.7$ we find $We=6.6$.

Carrying out the averaging described in Eq. (32), we obtain a correction to the value of the calculated frequency in Table 1. The corrected values are given in Table 1, in the fifth column. They are still above the experimental values but the trend in those, lower frequency for higher χ, is now present in the calculated values also.

7 Discussion

For a sphere the considered eigenmode is a spherical harmonic. The eigenmodes of ellipsoids have not been calculated analytically. In experiments frequencies are measured but not the eigenmodes, shape etc. The best reference is the beautiful paper [7] by Meiron, he calculated numerically a number of eigenmodes . His resulting frequencies are all of them higher than the experimental results in [6,8], as is shown in Fig. 3. For comparison we have included the pertinent values in Table 1. They are definitely closer to the experimental values than our results.

Meiron considered as we did a bubble rising in pure water. His calculation allows the bubble to assume a shape deviating from an ellipsoid. Indeed, it is known that a rising bubble has only approximately an ellipsoidal shape. In [1] it is shown by inspecting experimental results that there is an asymmetry about the equatorial plane. We suggest that this is the reason for the better fit of Meiron's [7] results.

An interesting approximation was introduced by Lunde and Perkins in [6]. They argued that for the (2,0) mode the wave length must be the distance from pole to pole , which is reasonable, and that the speed of the wave along the surface must be close to the speed of propagation of a capillary wave over a flat surface. These assumptions result for the (2,0) mode in

$$\omega = \left(\frac{16\sqrt{2}\chi^2}{(\chi^2+1)^{3/2}}\right)^{1/2}\left(\frac{\sigma}{\rho r_{\mathrm{eq}}^3}\right)^{1/2}. \tag{35}$$

The result in Eq. (35) fits, [6], rather well with experiments for χ about 2, shown in Fig. 3. This is very remarkable for two reasons. The first concerns taking for the wave speed the speed of a plane wave. One would expect that this is a good approximation when on the scale of a wave length the surface is flat, that means when the wave length is small with respect to the local radius of curvature. For the (2,0) mode this is by no means the case, near the equator the radius of curvature is on the contrary small with respect to the wave length. This observation is corroborated by applying (35) to a sphere for which the exact [10] value of ω is 3.46 $\sqrt{\sigma/\rho r_{\mathrm{eq}}^3}$, whereas the approximation of Eq. (35) gives 2.83 for the numerical factor, much farther off than for higher χ. Incidentally, our result, not corrected with E_v, gives 3.89. This is close to the exact value. Indeed, a sphere remains spherical only at zero rise velocity, so no correction is needed.

The second reason is that the energy due to the fluctuating vertical velocity, calculated in the present paper in Sect. 5, is not taken into account in the approximation leading to Eq. (35). It must therefore be considered as a (lucky) coincidence that the approximation represented by Eq. (35) works so well.

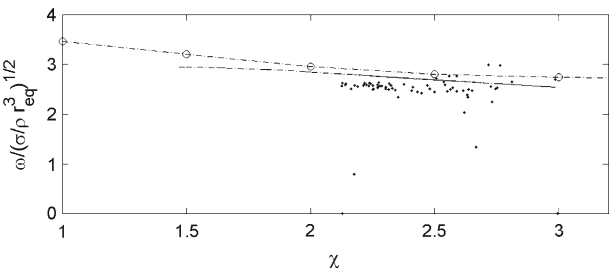

Fig. 3 Nondimensional frequency ω (rad/s) as a function of axes ratio χ. We are concerned with the upper data; *bullet* mode (2,0) from experiments [8], *circle with dash dotted line* Meiron's [7] results for (2,0) mode, *dash dotted line* aproximation, Eq. (35), by Lunde and Perkins [6]. From [8]

8 Volume oscillations of an ellipsoid

The oscillations with which we occupied ourselves in the previous sections are volume conserving. Gas filled bubbles can also perform volume oscillations. These are responsible for the emission of sound of streams and brooks [16], as well for the sound of rain on water [17]. In [16], a famous paper, Minnaert calculated the frequency of the breathing mode for a sphere. It is of interest to consider the breathing mode for an ellipsoid. The only paper that we have found on this subject is [18], by Strasberg. He used the fact that since we are dealing with potential flow, results from other fields governed by the potential equation may be used, as electrostatics or steady heat conduction. Working along this line, Strasberg could connect the problem of a breathing ellipsoid to that of finding the electric capacitance of such a shape. Using known results in that field, he calculated some value of the breathing frequency ω.

The solution of the potential equation represented in Eq. (6) that we used in previous sections represents a quadrupole. For the breathing mode we need the much simpler source solution. The solution for which

$$\frac{\dot{a}}{a} = \frac{\dot{c}}{c} = \frac{\dot{b}}{b}, \quad \text{and } a = b, \text{ is} \tag{36}$$

$$\phi = -\frac{1}{3} V \left(\frac{\dot{a}}{a} + \frac{\dot{c}}{2c} \right) \int_{\lambda}^{\infty} \frac{\mathrm{d}s}{F(s)}, \tag{37}$$

$F(s)$ being given by Eq. (7). This potential can be found in [11]. Working out the integral for $\lambda = 0$ results in the following expression on the ellipsoid:

$$\phi = V \frac{\dot{c}}{c^2} \left(\chi^2 - 1 \right)^{1/2} \frac{\cos^{-1} \chi^{-1}}{\chi}. \tag{38}$$

The kinetic energy can be calculated with help of Eq. (17). Inserting Eq. (38) into Eq. (17), we obtain for the kinetic energy E_o:

$$E_0 = \frac{2\pi\rho V}{(\chi^2 - 1)^{1/2}} (Vc)^{1/2} \left(\frac{\dot{c}^2}{c^2} \right) \cos^{-1} \chi^{-1}. \tag{39}$$

Next we calculate the potential energy

$$E_{\text{pot}} = \frac{4\pi}{3} \left\{ p_0 \left(V - V_0 \right) - \int_{V_0}^{V} p \mathrm{d}V \right\}. \tag{40}$$

Here V is as given in Eq. (3) whereas p denotes gas pressure, in equilibrium it has the value p_0. Under adiabatic behaviour and with ratio κ between specific heats, the right hand side of Eq. (40) can be easily evaluated. We

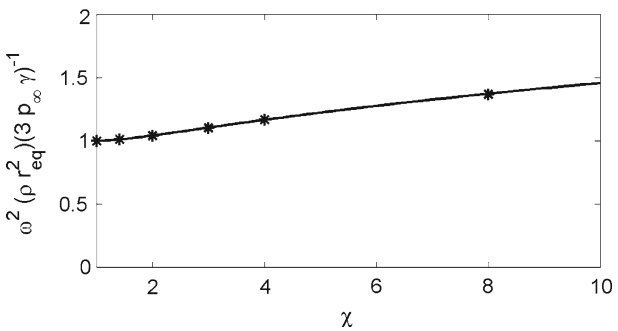

Fig. 4 Nondimensional frequency of volume oscillations (breathing mode) of ellipsoids as a function of the axes ratio χ. The *solid line* represents the right hand side of Eq. (42).The *'s are values calculated by Strasberg [18]

again vary c according to Eq. (4), but now change the other axes as prescribed in Eq. (36). Then we obtain to second order in $(c - c_0)$

$$E_{\text{pot}} = 6\pi\kappa p_0 V_0 \left(\frac{c - c_0}{c_0}\right)^2. \tag{41}$$

Taking again the perturbation $c - c_0$ as in Eq. (4), averaging the right hand sides of Eqs. (39) and (41) results in

$$\omega^2 = \frac{3\kappa p_0}{\rho r_{\text{eq}}^2} \frac{\left(\chi^2-1\right)^{1/2}}{\chi^{1/3}\cos^{-1}\chi^{-1}}. \tag{42}$$

For $\chi = 1$ the well known Minnaert frequency is recovered. For values $\chi > 1$, values as follow from Eq. (42) are presented in Fig. 4, together with values calculated in [18], both normalised with $(3\kappa p_0/\rho r_{\text{eq}}^2)$. Evidently, there is excellent agreement.

9 Conclusion

We have considered an ellipsoidal bubble performing an axisymmetrical oscillation whereby the minor axis fluctuates periodically, the volume remaining constant. Compared with the corresponding eigenmode as measured we find that the calculated values of the eigenfrequency are too high and also that they increase with the axes ratio of the undisturbed ellipsoid. We demonstrate that the latter discrepancy disappears when the energy fluctuation due to the fluctuating rise velocity is taken into account. We ascribe the first mentioned deviation from the experimental values to the fact that in reality a rising bubble is only approximately an ellipsoid.

In the final part of the paper we calculated the frequency of volume oscillations of ellipsoidal bubbles as a function of the axes ratio and we have compared our results with other works.

References

1. Duineveld, P.C.: The rise velocity and shape of bubbles in pure water at high Reynolds numbers. J. Fluid Mech. **292**, 325–332 (1995)
2. Mougin, G, Magnaudet, J.: Path instability of a rising bubble. Phys. Rev. Lett. **88**, 014502–014504 (2002)
3. de Vries, A.W.G., Biesheuvel, A., van Wijngaarden, L.: Notes on the path and wake of a gas bubble rising in pure water. Int. J. Multiphase Flow **28**, 1823–1835 (2002)
4. Ellingsen, K., Risso, F.: On the rise of an ellipsoidal bubble in water: oscillatory paths and liquid- induced velocity. J. Fluid Mech. **440**, 235–268 (2001)
5. Lindt, J.T.: On the periodic nature of the drag of a rising bubble. Chem. Eng. Sci. **27**, 1775–1781 (1972)
6. Lunde, K., Perkins, R.J.: Shape oscillations of rising bubbles. Appl. Sci. Res. **58**, 387–408 (1998)
7. Meiron, D.I.: On the stability of gas bubbles rising in in an inviscid fluid. J. Fluid Mech. **198**, 101–114 (1989)
8. Veldhuis, C.H.J.: Leonardo's Paradox, path and shape instabilities of particles and bubbles. Thesis University of Twente (2007)
9. Veldhuis, C., Biesheuvel, A., van Wijngaarden, L.: Shape-oscillations on bubbles rising in clean—and in tap-water. Phys. Fluids **40**, 046704–040716 (2008)
10. Lamb, S.H.: Hydrodynamics, 6th edn. Cambridge University Press, Cambridge, p. 475 (1932)
11. Milne-Thomson, L.M.: Theoretical Hydrodynamics, 2nd edn. Mac Millan, New York, pp. 453–454 (1949)
12. Bjerknes, C.A.: Verallgemeinerung des Problems von den Bewegungen, welche in einer ruhenden, unelastischen Flüssigkeit die Bewegung eines Ellipsoids hervorbringt. Nachrichten von der Königl. Gesellschaft der Wissenschaften und der G.A. Universität zu Gőttingen, vol. 80, pp. 829–867 (1873)
13. Benjamin, T.B.: Note on shape oscillations of bubbles. J. Fluid Mech. **203**, 419–424 (1989)
14. de Vries, J., Luther, S., Lohse, D.: Induced bubble shape oscillations and their impact on the rise velocity. Eur. Phys. J. B **29**, 503–509 (2002)
15. Van Wijngaarden, L., Kapteyn, C.: Concentration waves in dilute bubble/liquid mixtures. J. Fluid Mech. **212**, 111–137 (1990)
16. Minnaert, M.: Musical air bubbles and the sound of running water. Phil. Mag. **16**, 235–248 (1933)
17. Prosperetti, A., Oguz, H.: The impact of drops on liquid surfaces and the underwater noise of rain. Ann. Rev. Fluid Mech. **25**, 577–603 (1993)
18. Strasberg, M.: The pulsation frequency of nonspherical bubbles in liquids. J. Acoust. Soc. Am. **25**, 536–539 (1953)